

Performance of ILUT preconditioners in modeling bioheat and mass transfer in skin thermal injury

Wensheng Shen^a, Jun Zhang^{a,*}, Fuqian Yang^b

^aUniversity of Kentucky, Department of Computer Science, Lexington, KY 40508, USA

^bUniversity of Kentucky, Department of Chemical and Materials Engineering, Lexington, KY 40508, USA

Abstract

The transient heat and mass transfer in skin is investigated numerically using a finite difference method. Based on the skin physical structure, a three-dimensional multilayer model is developed and the governing equation is discretized using the Crank–Nicholson scheme. The resulting sparse linear system is solved by the generalized minimum residual method with an incomplete lower upper factorization with threshold (ILUT) preconditioner. The performance of the incomplete lower upper triangular factorization (ILUT) preconditioner is evaluated for different thresholds, solvers, and mesh sizes.

Keywords: Bioheat and mass transfer; Thermal injury; Crank–Nicholson scheme; Iterative method; ILUT preconditioning; Numerical modeling

1. Introduction

The effect of temperature change on skin thermal response may not be significant when the temperature at the skin surface is below 44 °C. However, if the surface temperature is above 44 °C, then irreversible damage may occur [1]. Very often, the related mass transfer, such as water evaporation and diffusion, is not considered in modeling the tissue response of high temperature exposure [2,3]. However, water transport may play an important role, and the heat loss due to the surface evaporation of water may become a dominant term in the heat transfer equation [4]. The objective of this work is to provide a quantitative connection between heating and the corresponding tissue thermal response with the consideration of water evaporation on the skin surface and water diffusion in the tissue.

The large-scale sparse linear system arising from the discretization of a three-dimensional (3D) partial differential equation (PDE) is solved iteratively. A Krylov subspace method, the generalized minimum residual (GMRES), is considered. An incomplete LU factorization with threshold (ILUT) preconditioner is used to achieve fast convergence and robustness.

2. Multilayer bioheat and mass transfer model

In the case that skin is subject to various heatings, the modified bioheat transfer equation may be written as [3,4]

$$\rho C \frac{\partial T}{\partial t} = k \frac{\partial^2 T}{\partial x^2} + k \frac{\partial^2 T}{\partial y^2} + k \frac{\partial^2 T}{\partial z^2} + w_b C_b (T_a - T) + Q \quad (1)$$

Where T is the temperature (in °C), T_a is the arterial temperature, and Q is the heat source. Note that the metabolic heat generation rate is neglected. The physical properties of the model related to Eq. (1) are summarized in Table 1.

The water transport in skin may be expressed by Fick's law of diffusion as [5]

$$\frac{\partial \rho_w}{\partial t} = D \left[\frac{\partial^2 \rho_w}{\partial x^2} + \frac{\partial^2 \rho_w}{\partial y^2} + \frac{\partial^2 \rho_w}{\partial z^2} \right] \quad (2)$$

where D is the coefficient of water diffusion in tissue (in m²/s), taken as $D = 5 \times 10^{-10}$ [4], and ρ_w is the corresponding water content (in g/m³).

The heat source Q in Eq. (1) may include the regional heat source Q_r , the volumetric heat loss of water evaporation Q_e , and the volumetric heat loss due to water diffusion Q_d , such that,

* Corresponding author. Tel.: +1 859 257 3892; Fax: +1 859 323 1971; E-mail: jzhang@cs.uky.edu

Table 1
Skin thickness and thermal physical properties used in this model

Property	Epidermis	Dermis	Subcutaneous	Blood
Thickness H (m)	8.0×10^{-5}	0.0020	0.010	
Thermal conductivity k (W/m K)	0.25	0.50	0.20	
Content ρ Kg/m ³	1200	1200	1000	1060
Specific heat C (J/kg K)	3600	3400	3000	3770
Blood perfusion rate w_b (m ³ /s/m ³ tissue)	0	0.00125	0.00125	
Absorption coefficient μ_a (mm ⁻¹)	80	2.4	1.0	
Initial water content W_0 (kg/m ³)	780	780	780	

$$Q = Q_r + Q_e + Q_d$$

where Q_r can be interpreted below if the heating source is of laser property,

$$Q_r = \mu_a \phi(x, y, z) f(t)$$

in which μ_a is the tissue absorption coefficient (1/m), $f(t)$ is the time function [6], and $\phi(x, y, z)$ is the local fluence rate of the laser light (in W/m²) [3],

$$\phi(x, y, z) = E \exp(-2(y^2 + z^2)/W^2) \exp(-\mu_a x)$$

where E is defined as $E = 2P/(\pi W^2)$, P is the laser power (in W), and W is the $1/e^2$ waist (in m).

The heat loss due to evaporation Q_e in Eq. (1) can then be expressed as [4]

$$Q_e = \dot{m} \Delta H_{vap}$$

where \dot{m} is the rate of water vaporization from the skin surface, and ΔH_{vap} is the enthalpy of vaporization of water, a function of temperature as tabulated in Lide [7]. The rate of water vaporization can be expressed as [4,8]

$$\dot{m} = \bar{D}_a \frac{M_w}{R} \frac{\left(\frac{P_w}{T_w}\right)_s - \left(\frac{P_w}{T_w}\right)_a}{\bar{\delta}_c} \times H_r$$

Here, \bar{D}_a is the average water vapor diffusivity in the boundary layer (in m²/s), H_r is the relative humidity of the air, M_w is the molecular weight of water (in g/mol), R the universal gas constant (in J/mol^oK), P_w is the vapor pressure of water (in Pa), and T_w is the temperature of the water vapor (in ^oK). $\bar{\delta}_c$ is the average thickness of the boundary layer over which a water vapor concentration gradient occurs. The average thickness of momentum boundary layer over the distance of L is found to be

$$\delta = \frac{10}{3} \sqrt{\frac{\nu L}{v_\infty}}$$

In the simulation, the dynamic viscosity of air ν and

the diffusivity of water vapor in air at a temperature of 25^oC are taken to be 1.57×10^{-5} m²/s and 2.6×10^{-5} m²/s, respectively [5]. The volumetric heat transfer rate due to water diffusion is then calculated as

$$Q_d = \frac{Dc_p(\rho_s - \rho_c)(T - T_c)}{(\Delta x)^2}$$

where c_p is the specific heat of water, ρ_s is the water content on the skin surface, ρ_c is the water content in the body core, T is the tissue temperature, and T_c is the temperature in the body core.

3. Numerical method and preconditioned iterative solver

Eqs (1) and (2) are discretized using the Crank–Nicholson scheme. Without losing generality, only the discretization of Eq. (1) is introduced here. Using the standard seven-point central finite difference approximation, the following expression can be derived:

$$\frac{T^{n+1} - T^n}{\Delta t} = \frac{1}{2} \alpha \mathcal{A} T^{n+1} + \frac{1}{2} \alpha \mathcal{A} T^n + S^{n+1/2} \quad (3)$$

Here, Δt is the time step, \mathcal{A} is the finite difference approximation of the elliptic operator, and S is the source term. The truncation error of the scheme is of order $\mathcal{O}(\Delta t^2 + h^2)$. Eq. (3) may be written in a matrix form, as follows:

$$\left(I - \frac{\alpha \Delta t}{2} \mathcal{A}\right) T^{n+1} = \left(I + \frac{\alpha \Delta t}{2} \mathcal{A}\right) T^n + \alpha \Delta t S^{n+1/2} \quad (4)$$

The sparse linear system, denoted by $Ax = b$ from Eq. (4), needs to be solved efficiently. One of the fastest iterative solvers, GMRES, is implemented with an ILUT preconditioner to solve the obtained linear system. The required storage grows quadratically with the number of iterations in a full implementation of GMRES. A restarted version of GMRES is employed as

GMRES(m), where m is the dimension of the Krylov subspace, so that GMRES is restarted after m iterations. The convergence rate of the GMRES method can be accelerated by preconditioned techniques. The idea of preconditioning is to solve an equivalent system $(M_L^{-1}AM_R^{-1})(M_Rx) = M_L^{-1}b$. Left or right preconditioning results, respectively, if $M_R = I$ or $M_L = I$. An ILUT is used to speed up the solution process. The ILUT preconditioner makes use of a dual dropping strategy that is represented by two parameters p and τ , where p is the number of fill-in elements and τ is the dropping tolerance. Detailed information about GMRES and ILUT can be found in Saad [9].

4. Numerical experiments

It is assumed that the skin under investigation is subject to laser heating every 0.1 s with a duration of 0.005 s for 2 s. The time step is chosen as $\Delta t = 0.001$ s, so that the laser heating is complete in five time steps in each period. Two different 3D mesh sizes have been considered, $49 \times 29 \times 29$ and $89 \times 49 \times 49$.

The numerical computations are conducted on a Sun Blade 100 workstation with a single 500-MHz Ultra-Sparc-IIe processor and 2 GB RAM. The performances of the linear system solver GMRES with a Krylov subspace size of 10 and the ILUT preconditioner for different combinations of p and τ are shown in Table 2. For all cases under consideration, the use of the ILUT preconditioner greatly reduces both the number of iterations and the total CPU time. The performance of ILUT depends very much on the combinations of the two parameters, the amount of fill-ins p and the dropping tolerance τ . The smaller the dropping tolerance, the fewer the number of iterations needed. After τ reaches a certain value, however, the number of iterations may not be reduced by decreasing τ . As shown in Table 2, the number of iterations is the same for $\tau = 10^{-3}$ and $\tau = 10^{-5}$, but more CPU time is needed in the latter case. The ILUT preconditioner is very efficient in reducing the computational cost in terms of saving overall CPU time for GMRES, but the average time needed for each iteration is larger in the case when the ILUT preconditioner is applied than that when the preconditioner is not used. The larger the mesh size, the more gains the ILUT preconditioner provides. For example, the total CPU time is reduced to nearly 1/2 and 1/4, respectively, for two different meshes when the ILUT preconditioner is used. According to Table 2, the optimal combination of the dual thresholds is $p = 15$ and $\tau = 10^{-3}$, in which the total CPU time is reduced from 128.41 s (without ILUT, mesh size $49 \times 29 \times 29$) to 54.16 s and from 1207.5 s (without ILUT, mesh size $89 \times 49 \times 49$) to 374.48 s.

Table 2

The performance of ILUT preconditioner for different parameters and mesh sizes

Size	p	τ	Iterations	ILUT	Solution
			62	N/A	128.41
$49 \times 29 \times 29$	5	10^{-1}	18	0.13	59.77
	5	10^{-3}	12	0.63	59.77
	5	10^{-5}	12	1.64	58.71
	15	10^{-1}	18	0.12	59.80
	15	10^{-3}	7	1.27	52.89
	15	10^{-5}	7	4.75	59.10
			124	N/A	1207.5
$89 \times 49 \times 49$	5	10^{-1}	29	0.63	425.79
	5	10^{-3}	18	3.83	376.58
	5	10^{-5}	18	12.73	385.62
	15	10^{-1}	29	0.63	425.42
	15	10^{-3}	10	9.95	364.53
	15	10^{-5}	10	37.75	395.14

A 3D temperature distribution of skin subject to a pulsed laser-heating under the consideration of water evaporation and diffusion is presented in Fig. 1, where the square at $x = 0.012$ m indicates the interface between epidermis and dermis layers, and the square at $x = 0.01$ m indicates the interface between the dermis and subcutaneous layers. As expected, an axisymmetrical temperature profile is obtained due to the heat source in Gaussian distribution, and the highest temperature is near the center of the region where it is heated. The same data have been used in both Figs 1a and 1b, but they are viewed from different angles. Fig. 1b is an anatomical view of the temperature distribution, from which the temperature variation on the three orthogonal planes is clearly shown. Numerical results without considering water evaporation or diffusion have also been obtained [6], but they are not presented here due to space limitations. It is clear that the skin surface temperature is reduced significantly if water evaporation and diffusion are considered. It is also reported [4] that water transport has greatly reduced the instant peak temperature and that water transport should be considered in modeling the skin thermal response.

5. Conclusion

A 3D multilayer model is proposed to investigate the transient thermal response of skin subject to laser heating; the impact of water evaporation and diffusion on skin temperature evolution are also included based on the laminar boundary-layer theory. Water transport

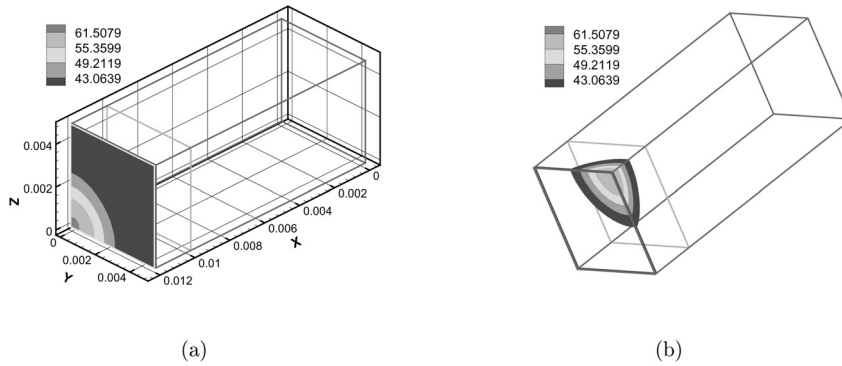


Fig. 1. 3D temperature distribution of the skin subject to external heating with Gaussian profile at $t = 2$ s: (a) viewed from the skin surface; (b) viewed anatomically to exhibit the temperature distribution on the three adjacent orthogonal planes.

moves a considerable amount of heat energy away from the skin, plays an important role in skin temperature evolution, and needs to be considered in modeling skin thermal response. The linear system is solved by GMRES with the ILUT preconditioner. It has been shown that ILUT is very efficient in accelerating the convergence rate of GMRES, and the optimal combination of p and τ for this problem is suggested based on our numerical experiments.

References

- [1] Moritz AR, Henriques FC. Studies of thermal injury II: the relative importance of time and surface temperature in the causation of cutaneous burns. *Am J Pathol* 1947;23:695–720.
- [2] Aguilar G, Choi B, Viator JA, Anderson D, Nelson JS. Experimental study of multiple-intermittent cryogen spurts and laser pulses for the treatment of port wine stain birthmarks. *IEEE Trans Biomed Engng* 2003;50:863–869.
- [3] Van Gemert MJC, Lucassen GW, Welch AJ. Time constants in thermal laser medicine: II. distributions of time constants and thermal relaxation of tissue. *Phys Med Biol* 1996;41:1381–1399.
- [4] Maitland DJ, Eder DD, London RA, Glinsky ME, Soltz BA. Dynamics simulations of tissue welding. *Proc SPIE* 1996;2671:234–242.
- [5] Welty JR, Wicks CE, Wilson RE, Rorrer GL. *Fundamentals of Momentum, Heat, and Mass Transfer*, 4th edn. New York: John Wiley & Sons, 2001.
- [6] Shen W, Zhang J, Yang F. Three-dimensional model on thermal response of skin subject to laser heating in soft tissue. Technical Report No. 409–04, Department of Computer Science, University of Kentucky, Lexington, KY, 2004.
- [7] Lide DR. *Handbook of Chemistry and Physics*, 74th edn. Boca Raton, FL: CRC Press, 1993.
- [8] Hisatake K, Tanaka S, Aizawa Y. Evaporation rate of water in a vessel. *J Appl Phys* 1993;73:7395–7401.
- [9] Saad Y. *Iterative Methods for Sparse Linear Systems*. New York: PWS Publishing, 1996.